RSC Advances

ROYAL SOCIETY OF CHEMISTRY

www.rsc.org/advances

RSC Advances

ARTICLE

Prussian blue modified metal–organic framework MIL-101(Fe) with intrinsic peroxidase-like catalytic activity as a colorimetric biosensing platform

Received 00th January 20xx,
Accepted 00th January 20xx

DOI: 10.1039/x0xx00000x

www.rsc.org/

Fengjuan Cui*, Qingfang Deng, Li Sun

In this paper, a nanosized porous PB/MIL-101(Fe), was facicly prepared with a uniform octahedral structure by growthing Prussian blue(PB) on microporous metal–organic framework MIL-101(Fe), and confirmed by cyclic voltammogram (CV), X-ray diffraction (XRD) and fourier transform infrared (FTIR) spectroscopy. It was demonstrated to possess intrinsic peroxidase-like activity and could catalytically oxidize 3,3′,5,5′-tetramethylbenzidine (TMB), *o*-phenylenediamine (OPD), and 2,2'-Azinobis-(3-ethylbenzthiazoline-6-sulphonate) (AzBTS) by H_2O_2 in solution to produce a typical coloured change. As a novel peroxidase mimic material, PB/MIL-101(Fe) shows high catalytic efficiency. Kinetic analysis of as the as-prepared PB/MIL-101(Fe) was studied, and they gave a linear absorbance response from 2.40 μM to 100 μM with a limit of detection (LOD) of 0.15 μM. It indicated that the catalytic behavior was consistend with typical Michaelis-Menten Kinetics and follows a ping-pong mechanism. Interstingly, the K_m values for PB/MIL-101(Fe) with respect to TMB and H_2O_2 is 0.127 and 0.0580 mM were lower than those of MIL-101(Fe) (0.490 and 0.620 mM for TMB and H_2O_2), respectively. This is probably attributed to more active sites and pore of the PB/MIL-101(Fe) for peroxidase substrates. More importantly, it can be easily functionalized with different compounds including silica coating (TEOS), 3-aminopropyltriethoxysilane (APTES), polyethylene glycol (PEG) or folic acid (FA) to make them biocompatible. The results reveal that the stability, ease of production and versatility of PB/MIL-101(Fe) nanoparticles could be used as a promising tool for cancer cell detection. With these findings, a simple and sensitive a colorimetric biosensing platform has been established.

Keywords: colorimetric biosensing; metal–organic frameworks; H_2O_2; peroxidase mimic;

1.Introduction

Metal–organic frameworks (MOFs) are organic-inorganic hybrid functional materials of coordination-bonded networks in which metal ions or metal ion clusters act as vertexes and organic ligands act as linkers [1-4]. Owing to the unique properties of these highly ordered crystalline materials such as large surface areas, high porosity, tunable pore sizes and topologies, as well as acceptable thermal stability, MOFs again received huge attention in the recently years as promising porous materials to explore their unparalleled potential for new applications including catalysis, drug delivery and imaging in life science research [2-10]. For instance, nanoscale or mesoscale MOF crystals have been successfully synthesized, which promote MOFs to act as carriers of drugs or bioactive compounds to target cellular or biological environments [11-17], and nanosized MOFs were integrated into electronic sensor devices to improve their performance in power sources [18-20]. So design and synthesis of new MOFs characterized with appropriate pore size, pore shape and pore surface functionality for bioanalysis is still fascinating. As known, postsynthetic modification (PSM) [21,22] can be considered as a controllable tool for MOFs functionalization without affecting the overall stability of the framework. The node-and-spacer model of these materials where coordinatively unsaturated metal center and organic ligands, makes them ideally suited for chemical manipulations to tailor the chemical stability and reactivity of the framework.

Take accounting to the new application in biosensing, three Fe(III)-based MOFs have been recently regarded as promising enzyme mimics reported in the literatures [23,24]. They show efficiently intrinsic peroxidase-like catalytic activity and can be established for colorimetric biosensing. Compared with natural enzymes, the MOFs-based enzyme mimics have many advantages, such as, highly stable, resistant to high substrate concentrations, low in cost, and easy to store and treat, thus they can provide particularly useful platforms and have been widely used in various fields including bioanalysis. Furthermore, peroxidase activity has a wide range of practical applications. For example, the ability to catalyze the oxidation of organic substrates to reduce their toxicity and/or to

College of Chemistry and Chemical Engineering, Qiqihar University, Qiqihar 161006, China.
† Corresponding authors.
Tel.: +86 452 2742575. E-mail address: cxf234@126.com.
Electronic Supplementary Information (ESI) available: [All the experiments concerning the catalytic activity of the MIL-101(Fe)] See DOI: 10.1039/x0xx00000x

produce a colour change is frequently used in wastewater treatment or as a detection tool [25-27]. So developing appropriate NMOFs-nanoparticles for peroxidase mimics is a practical approach. More recently reported about peroxidase-like enzyme mimics, all results show that two absorption peaks at 369 and 652 nm happened in the process of TMB oxidation. This can be ascribed to the charge-transfer complexes derived from the one-electron oxidation of TMB [28,29]. Thus, accelerating the electrons transform between catalysts and substrate maybe enhance catalytic activity of enzyme mimics.

Based on above mentioned idea, Prussian blue was successfully introduced into our enzyme mimics system. Prussian blue (PB) crystals consisting of iron ions coordinated by CN bridges are very typical coordination polymers with a high surface area, showing excellent properties in many applications such as catalysis, sensors, molecular magnets, gas storage [30-34]. Especially, PB exhibits high peroxidase-like catalytic activity for the reduction of hydrogen peroxide due to highly electroactivity [35,36]. However, owing to its limited dispersibility and functionalizability as well as its interfering strong blue color, PB has difficulty in applying for colorimetric biosensing in liquid solution.

In this work, we combine uniqueness of MIL-101(Fe) and PB to gain defect-driven PB/MIL-101(Fe) material via decorating with PB at the exposure metal sites on the MIL-101(Fe) in the process of synthesis. It show high efficiently peroxidase-like catalytic activity for the reduction of hydrogen peroxide like horseradish peroxidase (HRP) enzyme [37,38], the combining strategy take many advantages, such as, large reaction surface area, abundant sites accessible to substrates, and facile electron transfer (Scheme 1~~A~~). MIL-101(Fe), a Fe(III)-based MOF with molecular formula $Fe_3OH(H_2O)_2O[(BDC)]_3$, is one of materials of institute Lavoisier framework. It can be considered as Fe(III)-oxide clusters linked together in three dimensions by BDC linkers, which resulted from wide surface area and pore sizes[39]. As so far, MIL-101(Fe) was mostly selected as a host matrix not only because of its incredibly large pore size and high specific surface area but also because of its long term stability in water and air atmospheres. Furthermore, the exposed metal sites and ligands conveniently facilitate to achieve MOFs functionalization. However, MIL-101(Fe) as visible light photocatalysts because of their small band gap enabling visible light excitation has been reported as only one example in new application area [40], MIL-101(Fe) was used rarely as peroxidase mimetics for colorimetric biosensing. Here, the MIL-101(Fe) functioned as both a solid support as well as a Fe^{3+} source for PB growth and then formed uniform PB/MIL-101(Fe) octahedral nanostructures, which exhibited high efficiently catalytic activity for H_2O_2. PB is believed to bind to NMOF surface via multiple coordination bonds between CN residues on the PB backbone and vacant Fe^{3+} sites on the MIL-101(Fe) surface. Whereas the MIL-101(Fe) component will contribute to the expansion of the pore space, in which the adsorbate can be stored, and the presence of PB can increase the electron transform between catalysts and substrates.

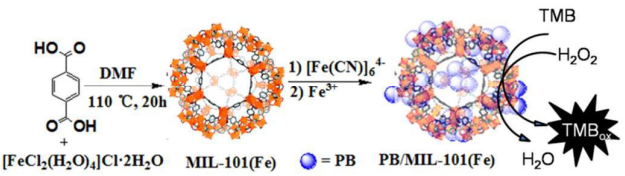

Scheme 1. Schematic illustration of synthesis PB/MIL-101(Fe) and using as a peroxidase mimetic

2. Experimental

2.1. Materials and Characterization

$FeCl_3{\cdot}6H_2O$, terephthalic acid (1,4-BDC), $K_4[Fe(CN)_6]$, dimethylformamide (DMF), acetic acid, sodium acetate (NaAc), H_2O_2 (30 wt%), 3,3',5,5'-tetramethylbenzidine dihydrochloride (TMB), 2,2'-Azinobis-(3-ethylbenzthiazoline-6-sulphonate) (AzBTS), o-phenylenediamine (OPD), tetraethylorthoilicate (TEOS), 3-aminopropyltriethoxysilane (APTES), polyethylene glycol (PEG-2000), and folic acid (FA) were purchased from Aladin Ltd. (Shanghai, China), unless otherwise noted, and used without further purification. All chemicals used in this study were of commercially available analytical grade.

Field emission scanning electron microscopy (FE-SEM) images were obtained with JEOL JSM 7401. The MIL-101(Fe) and PB/MIL-101(Fe) spheres were characterized by transmission electron microscope (TEM, H-7650B) at 80 kV. The EDS features of the samples were observed by high-revolution transmission electron microscope (HRTEM, JEOL, JEM-2010) operated at 120 kV. X-ray diffraction (XRD) characterization was carried out on a Bruker D8-Advance using Cu-Kα radiation (λ = 1.5418 Å). Fourier transform infrared spectra (FTIR) were recorded on Spectrum GX FTIR system. The Uv-Vis spectrums were characterized by HITACHI U-3900 spectrophotometer. All the experiments concerning the catalytic activity of the PB/MIL-101(Fe) were performed in triplicate and the data was analyzed using the graphics program Origin 8.0.

2.2. Preparation of PB/MIL-101(Fe) Composite

2.1.1. Preparation of Metal-Organic Framework MIL-101(Fe)

MIL-101(Fe) was prepared following the protocol described earlier [41]. In a typical synthesis, a mixture of 0.675 g (2.45 mmol) of $FeCl_3{\cdot}6H_2O$, 0.206 g of H_2BDC (1.24 mmol), and 15 mL DMF was heated at 110 °C for 20 h in a Teflon-lined stainless steel bomb. The resulting brown solid was filtered off and the raw product was purified by a double treatment in ethanol at 60 °C for 3 h. Activated MIL-101(Fe) was obtained by drying under vacuum at 120 °C for 7 h before using.

2.2.2. Preparation of PB/MIL-101(Fe) Composite

First, owing to the as-prepared metal-organic framework MIL-101(Fe) has a lot of hydrophilic pores on the surface, the $[Fe(CN)_6]_4$/MIL-101(Fe) precursors was carried out using double solvents method [42]. Typically, 0.050 g of dehydrated MIL-101(Fe) was suspended in 40 mL of dry n-hexane as hydrophobic solvent and the mixture was sonicated for about 20 min until it became homogeneous. After stirring for a while, 1 mL of 100 mM aqueous $K_4[Fe(CN)_6]$ solution as the hydrophilic solvent was added dropwise over a period of 10

min with constant vigorous stirring. The resulting solution was continuously stirred for 3 h at room temperature. After stirring, the solid which settled down to the bottom of the sample vial was isolated from the supernatant by decanting, washing several with water and drying in air at room temperature. The synthesized sample was further dried at 120 °C under vacuum for 12 h.

Second, the $[Fe(CN)_6]_4$/MIL-101(Fe) precursors were redispered in 40 mL of dry n-hexane and the mixture was sonicated for about 20 min until it became homogeneous. After stirring for a while, 1 mL of 100 mM aqueous $FeCl_3$ solution as the hydrophilic solvent was added dropwise over a period of 20 min with constant vigorous stirring. The resulting solution was continuously stirred for 3 h at room temperature. After stirring, the solid which settled down to the bottom of the sample vial was isolated from the supernatant by decanting, washing several with water and drying in air at room temperature. The synthesized sample was further dried at 60 °C under vacuum for 12 h.

2.3. Bioassay

2.3.1 Detection of H_2O_2 using PB/MIL-101(Fe).

To investigate the peroxidase-like activity of the as-prepared PB/MIL-101(Fe), the catalytic oxidation of the peroxidase substrate TMB in the presence of H_2O_2 was tested. The measurements were carried out by monitoring the absorbance change of TMB at 652 nm. In a typical experiment, 20 µL PB/MIL-101(Fe) dispersion (final concentration 0.2 mg mL^{-1}) were mixed in 50 µL of NaAc buffer solution (pH 5.0), followed by adding 20 µL of TMB solution (final concentration 0.2 mM, NaAc buffer solution (pH 5.0)). Then, 10 µL of H_2O_2 of various concentrations was added into the mixture. The mixed solution was incubated at 37 °C for 2 min for standard curve measurement.

2.3.2 Detection of glucose using PB/MIL-101(Fe).

Glucose detection was performed as follows: a) 0.1 mL of 1 mg/mL GOx and 20 µL PB/MIL-101(Fe) dispersion (final concentration 0.2 mg mL-1) in 0.5 mL of NaAc buffer solution (pH 5.0) were incubated at 37 °C for 30 min; b) 50 µL of glucose of different concentrations were added to the above solution ; and c) the mixed solution was incubated at 37 °C for 5 min and then for standard curve measurement.

3. Results and discussion

3.1. Preparation and characterization of PB/MIL-101(Fe) composite

MIL-101(Fe) is made from inexpensive and biocompatible iron(III) and terephthalic acid (BDC) by a facile one-pot solvothermal method using DMF as solvent in a Teflon-lined bomb according to the reported approaches (Electronic Supplementary Information, ESI). It shows very good stability. And then the MIL-101(Fe) was activated via heating for further used. PB/MIL-101(Fe) was synthesized using double solvents method (Electronic Supplementary Information, ESI). According to the XPS and elemental analysis experiment, the formula is $KFe(III)[Fe(CN)_6]Fe_2(III)(OH)(DMF)O(BDC)_3$, the XPS results as shown in Fig S2 and S3(ESI), it show that the iron in the PB/MIL-101(Fe) have two species, Fe(II) and Fe(III), and the ratio Fe(II) to Fe(III) is 1:3. BET surface area measurement as Fig. S4, the specific surface area of MIL-101(Fe), measured by the Brunauer Emmett Teller (BET) method, is 1469.1 m^2/g. The surface area of the PB/MIL-101(Fe) is 1649.8 m^2/g, larger than that of MIL-101(Fe). The relatively high surface area indicates that most of the MOF surface is connected by the PB.

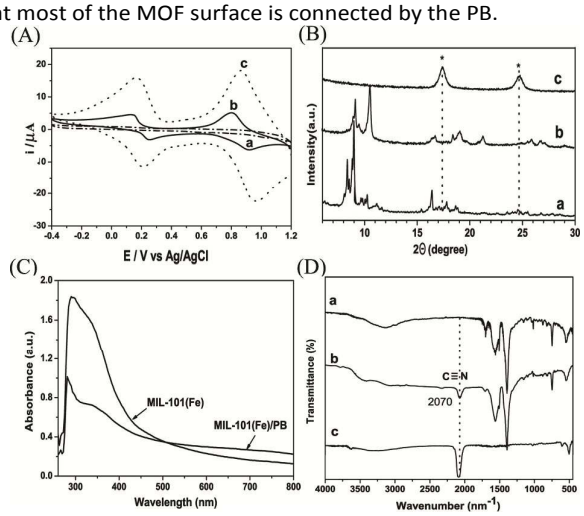

Figure 1. (A) Cyclic voltammogram of the MIL-101(Fe) (a), PB/MIL-101(Fe) (b) and PB modified GCE (c) in a 0.05 M pH 6.0 PBS (contain 0.1 M KCl) solution with a scan rate of 50 mV/s; (B) PXRD patterns of as-prepared MIL-101(Fe) (a), as-prepared PB/MIL-101(Fe) (b) and PB (c); (C) UV/Vis spectra of PB/MIL-101(Fe) and MIL-101(Fe) suspension with concentration of 0.2 mg/mL in a pH 5.0 acetate buffer; (D) FTIR spectrum of MIL-101(Fe) (a), PB/MIL-101(Fe) (b), and PB (c).

The formation of PB/MIL-101(Fe) assemblies is further supported by the following observations. Upon PB loading, the color of the MOF powders changed from reddish-orange to yellowish-green due to the visible absorption of PB. Due to the high electroactivity of PB, PB/MIL-101(Fe) was first examined by a cyclovoltammetric (CV) method with a PB/MIL-101(Fe)-modified glassy carbon electrode (GCE) in pH 6.0 phosphate buffer solution (PBS). For comparison, a PB/MIL-101(Fe)-modified GCE electrode (PB/MIL-101(Fe)/GCE) show similar electro-behavior with PB on GCE electrode (PB/GCE) (Figure 1A), while the MIL-101(Fe)/GCE electrode showed no redox peak. The PB/MIL-101(Fe)/GCE electrode showed redox peaks at 0.24/0.15 V, which correspond to the inter conversion between Prussian white and PB, and peaks at 0.92/0.80 V corresponding to the inter conversion between PB and Berlin green [43,44].

PXRD patterns of PB/MIL-101(Fe) showed that the framework structure of MIL-101(Fe) was maintained good crystalline (Figure 1B). On the other hand, peaks in the PXRD patterns of PB/MIL-101(Fe) happened to obviously shift, indicating Fe^{2+} in PB interacted with the Fe^{3+} of MIL-101(Fe) by [Fe^{2+}–CN–Fe^{3+}] bond and formed the product. However, the peaks of PB is absent for PB/MIL-101(Fe) due to shielding by the MIL-101(Fe), meanwhile we can also see that the peaks at 17.5 and 24.8 ° of MIL-101(Fe) disappeared because of the formation of PB. UV-vis absorption spectra (Figure 1C) also are present MIL-101(Fe) and PB/MIL-101(Fe). In the case of

modified PB/MIL-101(Fe) particles, very wide absorption peak could be observed at a range of 500-800 nm and strengthen, which attributed to the mixed-valence charge-transfer band at 700 nm of the polymeric [Fe^{2+}–CN–Fe^{3+}] sequence as the literature previously reported [45], while the peak of ligands in the range of 300-400 nm decreased due to the surface covered by newly formed PB. The FTIR absorption spectra (Figure 1D) give a comparison between PB/MIL-101(Fe) and MIL-101(Fe). The spectrum of the PB/MIL-101(Fe) exhibited a peak at 2070 cm^{-1} attributed to the CN stretching in the formed [Fe^{2+}–CN–Fe^{3+}] structure, which indicates the PB formation on the surface of MIL-101(Fe) [46]. The chemical composition determined by the EDS spectrum (Fig. S1, ESI) reveals that the C, Fe, O and N elements coexist in PB/MIL-101(Fe). The PB formation was consistent with the UV-vis and FTIR spectrum indicating the fact that MIL-101(Fe) NPs were modified with PB.

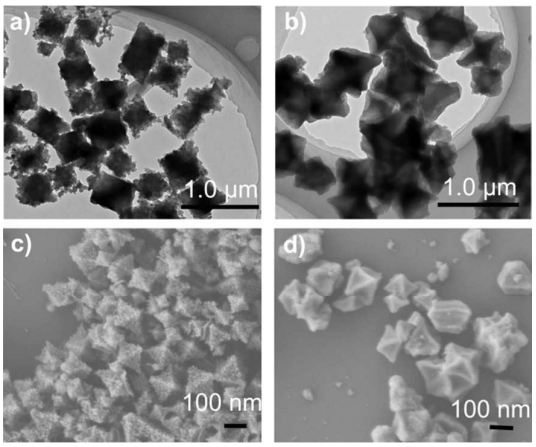

Figure 2. TEM images (a, b), SEM images (c, d), of MIL-101(Fe) (a, c) and PB/MIL-101(Fe) (b, d).

The morphology and structural features of as-prepared MIL-101(Fe) precursor and PB/MIL-101(Fe) were characterized by transmission electron microscopy (TEM) and scanning electron microscopy (SEM). Before modification, TEM and SEM show the MIL-101(Fe) precursor consists of uniform octahedral nanostructures with an average edge length of ca. 350 nm, rough surface, indicating that these octahedral nanostructures are constructed by many small pores on the surface (Figure 2a, 2c). After modification with PB, the SEM and TEM images show that the uniform octahedral nanostructures tend to be slightly larger, more smoothing on the surface and the edge length is approximately 500 nm for PB/MIL-101(Fe) (Figure 2b, 2d). This may be due to the PB grow up in the small pores on the surface of MIL-101(Fe) through the CN of PB coordinating with the Fe^{3+} in MIL-101(Fe), and then the surface of MIL-101(Fe) go into smoothing thus formed PB/MIL-101(Fe). The obtained PB/MIL-101(Fe) could be stably dispersed in aqueous solution. Finally, the content of PB in PB/MIL-101(Fe) was evaluated by gravimetric method (see the Supporting Information S3 section Table S1) and obtained a percentage of (10.34±0.31) % PB on PB/MIL-101(Fe).

3.2.Sensing applications of PB/MIL-101(Fe)

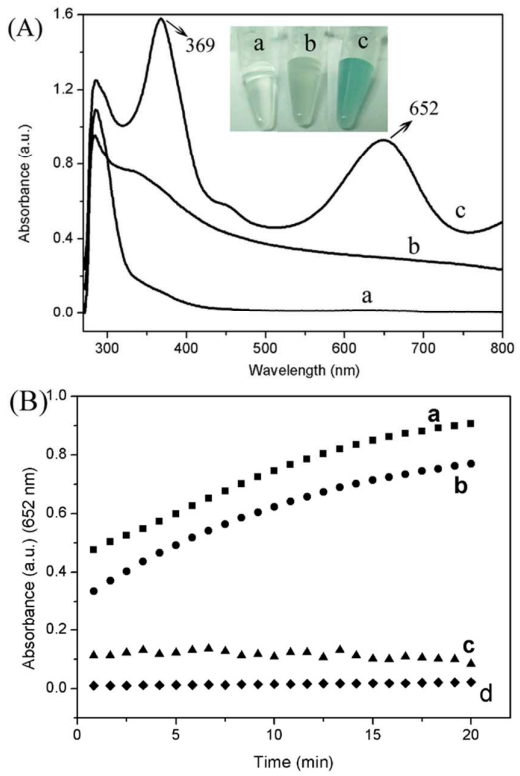

Figure 3. (A) UV/Vis spectra of TMB and H_2O_2 (a), PB/MIL-101(Fe) suspension (b), TMB, H_2O_2, and PB/MIL-101(Fe) (c) in a pH 5.0 acetate buffer at 37 °C for 2 min. [TMB]: 1 mM, [H_2O_2]: 1 mM, [PB/MIL-101(Fe)]: 0.2 mg mL-1. Inset shows corresponding photographs. (B) UV-vis adsorption intensities at 652 nm in the first 20 minutes record the oxidation process of TMB in the presence PB/MIL-101(Fe) (a), MIL-101(Fe) (b), PB (c) or absence of MOF catalysts (d).

Recently, colorimetric biosensing in biological science and analytical chemistry due to its simplicity, rapidity, direct visual readout has been received widespread attention. The peroxidase-like activity of PB/MIL-101(Fe) was evaluated by the catalytic oxidation of peroxidase substrate TMB in the presence of H_2O_2. As shown in Figure 3A, in the presence of H_2O_2, a colorless TMB solution was observed, which displayed a negligible absorption in the range 350 to 700 nm, indicating that no oxidation reaction occurred in the absence of PB/MIL-101(Fe). In contrast, when PB/MIL-101(Fe) was introduced into the solution, a typical deep-blue color was observed in the reaction mixture, and the solutions exhibited intense characteristic absorbance at 369 and 652 nm (Figure 3A) in the UV-vis spectra. The phenomenon is similar to that observed for the commonly used horseradish peroxidase (HRP) enzyme. Similar to HRP, the catalytic activity of PB/MIL-101(Fe) is dependent on temperature, pH value, H_2O_2 concentration and catalyst concentration. We measured PB/MIL-101(Fe) peroxidase like activity while varying: 1) pH from 2 to 7, 2) temperature from 20 to 50 °C, and 3) H_2O_2 concentration from 0.3 M to 80 mM(Fig. S6). Under our experimental conditions, the optimal pH is 5.0 for PB/MIL-101(Fe) and the best temperature is approximately 37 °C, which are similar to the values for other nanostructured peroxidase mimetics and HRP

[22,25], All these observations reveal that PB/MIL-101(Fe) has peroxidase like catalytic ability and they can catalyze the oxidation of TMB in the presence of H_2O_2. They also exhibited high catalytic activity for other peroxidase substrates, such as o-phenylenediamine (OPD), 2,2'-Azinobis-(3-ethylbenzthiazoline-6-sulphonate) (AzBTS) in the presence of H_2O_2 (Fig. S8).

In order to avoid the observed activity resulted from the leaching of iron ions in acidic condition, we incubated PB/MIL-101(Fe) in the standard reaction buffer (pH 5.0) for 2 min and then removed the PB/MIL-101(Fe) from solution with a separation. We then compared the activity of the leaching solution and Fe^{3+} as catalyst with that of PB/MIL-101(Fe) under the same conditions. As shown in Figure S9, the leaching solution had no activity, meanwhile high concentration of Fe^{3+} also exhibited different enzyme activity but still lower than PB/MIL-101(Fe), showing that the PB/MIL-101(Fe) peroxidase-like enzyme keep intact in the whole process of catalytic reaction. Furthermore, in the control experiments (Figure 3B), PB/MIL-101(Fe) show more highly catalytic activity than that of MIL-101(Fe), which proposed that by incorporating PB into MIL-101(Fe), the peroxidase like catalytic ability enhance significantly, due to the fast electron transfer effect of PB. FT-IT, TEM, SEM and PXRD results show the phase structure of PB/MIL-101(Fe) unchanged after peroxidase reaction. (Fig. S9-11, ESI). All results further demonstrated the integrity between PB and MIL-101(Fe) to enhance peroxidase-like catalytic activity.

The peroxidase-like catalytic activities of MIL-101(Fe) and PB/MIL-101(Fe) were evaluated by means of steady-state kinetics by changing the concentration of TMB and H_2O_2 in the system (Fig. S12, ESI). Typical Michaeli-Menten curves were obtained by monitoring the absorbance change at 652 nm for 2 min. Michaeli-Menten constant K_m and maximum initial rate V_{max} were obtained from a Line weaver-Burk plot [47]. We found that catalysis by PB/MIL-101(Fe) followed typical Michaelis-Menten behavior towards TMB and H_2O_2 (Fig. S12, Table S3). The apparent K_m values for PB/MIL-101(Fe) with respect to TMB and H_2O_2 is 0.127 and 0.0580 mM respectively were lower than those of MIL-101(Fe) (0.490 and 0.620 mM for TMB and H_2O_2, respectively; Table S3 in the Supporting Information) and suggest that PB/MIL-101(Fe) has a higher affinity to TMB and H_2O_2 than MIL-101(Fe), since it is well known that a smaller K_m value implies higher enzyme–substrate affinity [31]. It is not difficult to understand, the PB brought more active iron sites substrates.

The catalytic mechanism of PB/MIL-101(Fe) was further investigated by the detection of in situ-generated hydroxyl radicals (·OH) with a photoluminescence (PL) method [23]. A gradual increase in PL intensity at about 425 nm was observed with increasing PB/MIL-101(Fe) concentration (Fig. S13). Notably, there was no PL intensity in the absence of PB/MIL-101(Fe). This confirms that PB/MIL-101(Fe) can catalytically activate H_2O_2 to produce ·OH radicals, which could then react with TMB to produce a color change in the reaction. It is believed that the peroxidase-like activity of PB/MIL-101(Fe) could originate from its catalytic activation of H_2O_2 through electron transfer to produce ·OH radicals by a Fenton-like reaction [24].

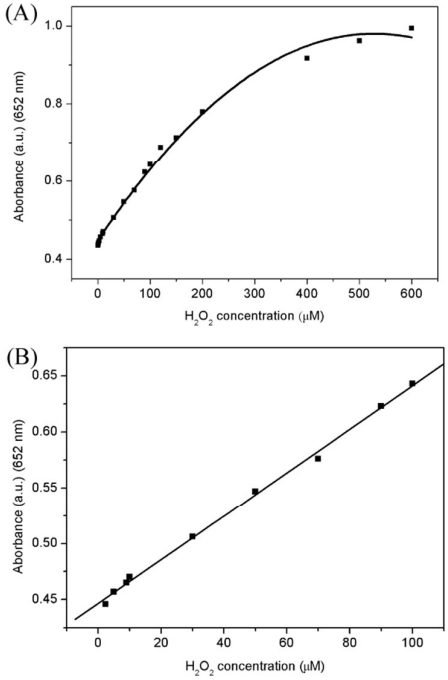

Figure 4. (A) A dose-response curve for H_2O_2 detection using PB/MIL-101(Fe) under the optimum conditions described; (B) linear calibration plot for H_2O_2.

Given the intrinsic peroxidase properties of PB/MIL-101(Fe), a colorimetric method for detection of H_2O_2 using PB/MIL-101(Fe) catalyzed blue color change was established. Figure 4 shows the dependence of the absorbance at 652 nm on the concentration of H_2O_2 under optimal conditions (i.e., pH 5.0, 37 °C). The absorbance at 652 nm increases with increasing H_2O_2 concentration from 0.3 μM to 600 μM. A linear relationship (Figure 4B) between the absorbance and the H_2O_2 concentration between 2.4 to 100 μM (R^2 = 0.998) was obtained, with a detection limit of 0.15 μM, which is comparable with that now available MOFs nanoparticles [23,24]. Furthermore, the colour variation is obvious on visual observation, offering a convenient approach to detect H_2O_2 by the naked eye even at low concentrations.

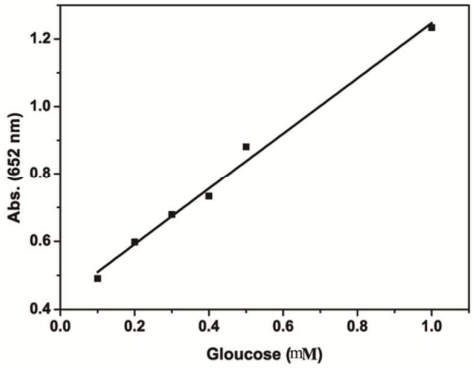

Figure 5. The response curves of glucose.

When combined with glucose oxidase (GOx), the proposed colorimetric method could be used for the determination of glucose, which is an important indicator for the diagnosis of diabetes mellitus in clinical medicine [48]. Figure 5 shows the standard curve of the glucose response. The linear range for glucose was from 0.1 to 1.0 mM and the DL was as low as 0.4 μM. Fructose, lactose, and maltose were used to investigate the selectivity of this biosensing system. The results (Fig. S5, ESI) demonstrated that the absorbance of these glucose analogues was negligible compared with that of glucose even at concentrations as high as 5 mM. This indicates that this biosensing system has high selectivity for glucose, which could be attributed to the high affinity of glucose oxidase for glucose [49].

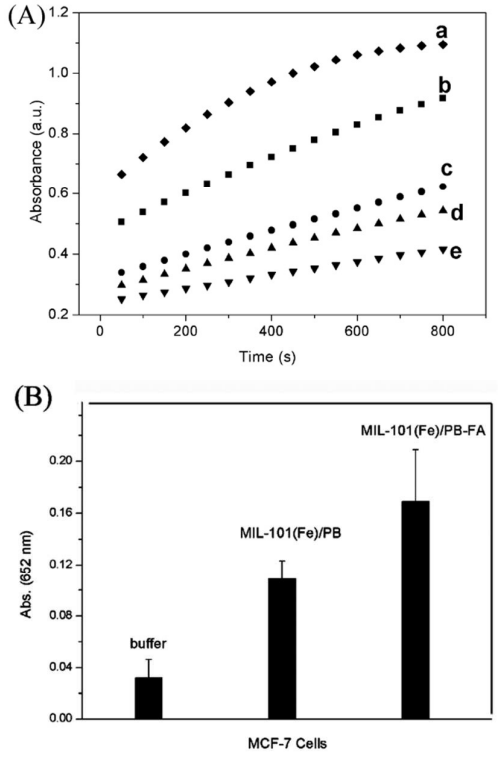

Figure 6. (A) UV-vis adsorption intensities at 652 nm in the first 15 minutes record the oxidation process of TMB in the presence of a) PB/MIL-101(Fe) and modified with b) silica coating, c) amino modification, d) PEG, e) FA. (B) Detection of folate receptor expressing 5×10^4 MCF-7 cells (from left to right: buffer, PB/MIL-101(Fe), PB/MIL-101(Fe)-FA).

We also modified the PB/MIL-101(Fe) with different compounds including tetraethylorthosilicate (TEOS), 3-aminopropyltriethoxysilane (APTES), polyethylene glycol (PEG) and folic acid (FA) to make them biocompatible. PB/MIL-101(Fe)-coated could be easily synthesized by absorption of coating reagents onto the PB/MIL-101(Fe) because of the exposed iron sites and carboxyl groups on the surface of PB/MIL-101(Fe). The as prepared PB/MIL-101(Fe)-coated was confirmed by UV/Vis and FTIR measurements (Fig. S14, ESI). In the UV/Vis spectra, a peak at 500-700 nm is obviously decreased due to the coverage of coating on PB/MIL-101(Fe). As observed, the enzyme activity decreased after modification compared with the original PB/MIL-101(Fe), which can be ascribed to coating layers shield the active sites from the substrate and hence affect activity (Figure 6A).

As known, folic acid was one of the most commonly employed small molecules, which could target the folate receptor present on the surface of tumor cells [44,45]. So we tested PB/MIL-101(Fe)-FA as a probe for fast colorimetric detection of cancer cells. PB/MIL-101(Fe)-FA and PB/MIL-101(Fe) were respectively incubated with MCF-7 cells in EMDM medium for 1.5 hours and subsequently centrifuged. The precipitate was collected and rinsed with PBS three times to remove the unattached catalysts. In the presence of TMB and H_2O_2, the absorbance changes at 652 nm can be monitored by Uv-Vis. Following 1.5 h in culture, PB/MIL-101(Fe)-FA expressed much stronger binding to MCF-7 cells than that of PB/MIL-101(Fe) (Figure 6B). As the number of MCF-7 cells increased, the absorbance changed, that suggests that more PB/MIL-101(Fe) bind to folate receptors on the surface of MCF-7cells (Fig. S15).

Conclusions

In summary, we have prepared PB/MIL-101(Fe) nanocomposites as a novel peroxidase mimic to develop colorimetric sensing protocols for H_2O_2. PB/MIL-101(Fe) was used for colorimetric determination of H_2O_2 with a linear range from 2.40 μM to 100 μM with a limit of detection (LOD) of 0.15 μM. Moreover, the outer surfaces of PB/MIL-101(Fe) were exploited to anchor biocompatible molecule and remain high activity. It may be further used as enzymatic mimics for potential applications in immunoassays, medical diagnostics and biotechnology in future.

Acknowledgements

This work was financially supported by the National Basic Research Program of China (No. 2011CB935700), the Postdoctoral Scientific Research Developmental Fund (No. LBH-Q14158) and the Program for Yong Teachers Scientific Research in Qiqihar University (No. 2014k-Z07). The author thanks Pro. Jinghong Li, Tsinghua University and Dr. Lei Xu, Qiqihar University for help.

Notes and references

1 H. Furukawa, K.E. Cordova, M. O'Keeffe and O.M. Yaghi, *Science,* 2013, **341**, 974.
2 D. Yan, Y. Tang, H. Lin and D. Wang, *Sci. Rep.,* 2014, **4**, 4337.
3 M. Sindoro, N. Yanai, A.Y. Jee and S. Granick, *Acc. Chem. Res.,* 2014, **47**, 459.
4 P. Horcajada, R. Gref, T. Baati, P.K. Allan, G. Maurin, P. Couvreur, G. Ferey, R.E. Morris and C. Serre, *Chem. Rev.,* 2012, **112**, 1232.
5 P. Horcajada, T. Chalati, C. Serre, B. Gillet, C. Sebrie, T. Baati, J.F. Eubank, D. Heurtaux, P. Clayette, C. Kreuz, J.S. Chang, Y.K. Hwang, V. Marsaud, P.N. Bories, L. Cynober, S. Gil, G. Férey, P. Couvreur and R. Gref, *Nat. Mater.,* 2010, **9**, 172.

6 A.C. McKinlay, R.E. Morris, P. Horcajada, G. Ferey, R. Gref, P. Couvreur and C. Serre, *Angew. Chem. Int. Ed.,* 2010, **49**, 6260.
7 J. Lee, O.K. Farha, J. Roberts, K.A. Scheidt, S.T. Nguyen and J.T. Hupp, *Chem. Soc. Rev.,* 2009, **38**, 1450.
8 Y. Cui, Y. Yue, G. Qian and B. Chen, *Chem. Rev.,* 2012, **112**, 1126.
9 J. Song, Z. Luo, D.K. Britt, H. Furukawa, O.M. Yaghi, K.I. Hardcastle, and C.L. Hill, *J. Am. Chem. Soc.,* 2011, **133**, 16839.
10 V.P. Santos, T.A. Wezendonk, J.J.D. Jaén, A.I. Dugulan, M.A. Nasalevich, H.-U. Islam, A. Chojecki, S. Sartipi, X. Sun, A.A. Hakeem, Ard C.J. Koeken, M. Ruitenbeek, T. Davidian, G.R. Meima, G. Sankar, F. Kapteijn, M. Makkee and J. Gascon, *Nature Communications.* 2015, **6**, doi: 10.1038/ncomms7451.
11 K.M.L. Taylor, W.J. Rieter and W. Lin, *J. Am. Chem. Soc.,* 2008, **130**, 14358.
12 W.J. Rieter, K.M.L. Taylor and W. Lin, *J. Am. Chem. Soc.,* **129**, 9852.
13 J.D. Rocca, D. Liu and W. Lin, *Acc. Chem. Res.,* 2011, **44**, 957.
14 M. Jahan, Q. Bao, J.X. Yang and K.P. Loh, *J. Am. Chem. Soc.,* 2010, **132**, 14487.
15 W. Dong, X. Liu, W. Shi and Y. Huang, *RSC Adv.*, 2015, **5**, 17451.
16 E.-L. Zhou, C. Qin, P. Huang, X.-L. Wang, W.-C. Chen, K.-Z. Shao and Z.-M. Su, *Chem. Eur. J.*, 2015, **21**, 11894.
17 Z. Jiang, Y. Liu, X. Hua and Y. Li, *Anal. Methods*, 2014, **6**, 5647.
18 M. Jahan, Q. Bao and K.P. Loh, *J. Am. Chem. Soc.,* 2012, **134**, 6707.
19 C. Hou, J. Peng, Q. Xu, Z. Ji and X. Hu, *RSC Adv.,* 2012, **2**, 12696.
20 A. Morozan and F. Jaouen, *Energy Environ. Sci.,* 2012, **5**, 9269.
21 K.K. Tanabe and S.M. Cohen, *Chem. Soc. Rev.,* 2011, **40**, 498.
22 S.M. Cohen, *Chem. Rev.,* 2012, **112**, 970.
23 L. Ai, L. Li, C. Zhang, J. Fu and J. Jiang, *Chem. Eur. J.,* 2013, **19**, 15105.
24 J.W. Zhang, H.T. Zhang, Z.Y. Du, X. Wang, S.H. Yu and H.L. Jiang, *Chem. Commun.,* 2014, **50**, 1092.
25 H. Wei and E.K. Wang, *Chem. Soc. Rev.,* 2013, **42**, 6060.
26 W. Shi, Q. Wang, Y. Long, Z. Cheng, S. Chen, H. Zheng and Y. Huang, *Chem. Commun.,* 2011, **47**, 6695.
27 Y. Chen, H. Cao, W. Shi, H. Liu and Y. Huang, *Chem. Commun.,* 2013, **49**, 5013.
28 24 X. Sun, S. Guo, C.S. Chung, W. Zhu and S. Sun, *Adv. Mater.,* 2013, **25**, 132.
29 P.D. Josephy, T. Eling and R.P. Mason, *J. Biol. Chem.,* 1982, **257**, 3669.
30 L. Wang, Y. Ye, H. Zhu, Y. Song, S. He, F. Xu and H. Hou, *Nanotechnol.*, 2012, **23**, 455502.
31 M. Hu, S. Ishihara and Y. Yamauchi, *Angew. Chem. Int. Ed.,* 2013, **52**, 1235.
32 D.M. Pajerowski, J.E. Gardner, F.A. Frye, M.J. Andrus, M.F. Dumont, E.S. Knowles, M.W. Meisel and D.R. Talham, *Chem. Mater.,* 2011, **23**, 3045.
33 K. Sone, K. Konishi and M. Yagi, *Chem. Eur. J.,* 2006, **12**, 8558.
34 N.R. Tacconi and K. Rajeshwar, *Chem. Mater.,* 2003, **15**, 3046.
35 T. Wang, Y. Fu, L. Chai, L. Chao, L. Bu, Y. Meng, C. Chen, M. Ma, Q. Xie and S. Yao, *Chem. Eur. J.,* 2014, **20**, 2623.
36 T. Wang, Y. Fu, L. Bu, C. Qin, Y. Meng, C. Chen, M. Ma, Q. Xie and S. Yao, *J. Phys. Chem. C*, 2012, **116**, 20908.
37 N.C. Veitch, *Phytochem.,* 2204, **65**, 249.
38 L.Z. Gao, J. Zhuang, L. Nie, J.B. Zhang, Y. Zhang, N. Gu, T.H. Wang, J. Feng, D. L. Yang, S. Perrett and X.Y. Yan, *Nat. Nanotechnol.,* 2007, **2**, 577.
39 O.V.Z. Nataliya V. Maksimchuk, I.Y. Skobelev, A. Konstantin and A.K. Kovalenko, *Proc. R. Soc. A,* 2012, **468**, 2017.
40 K.G. Laurier, F. Vermoortele, R. Ameloot, D.E. De Vos, J. Hofkens and M.B. Roeffaers, *J. Am. Chem. Soc.,* 2013, **135**, 14488.
41 K.M.L. Taylor-Pashow, J.D. Rocca, Z. Xie, S. Tran and W. Lin, *J. Am. Chem. Soc.,* 2009, **131**, 14261.
42 Q.L. Zhu, J. Li and Q. Xu, *J. Am. Chem. Soc.,* 2013, **135**, 10210.
43 D. Du, M. Wang, Y. Qin and Y. Lin, *J. Mater. Chem.,* 2010, **20**, 1532.
44 Z. Li, J. Chen, W. Li, K. Chen, L. Nie and S. Yao, *J. Electroanal. Chem.,* 2007, **603**, 59.
45 M. Taguchi, I. Yagi, M. Nakagawa, T. Iyoda and Y. Einaga, *J. Am. Chem. Soc.,* 2006, **128**, 10978.
46 S. Choudhury, N. Bagkar, G.K. Dey, H. Subramanian and J.V. Yakhmi, *Langmuir,* 2002, **18**, 7409.
47 H. Lineweaver and D. Burk, *J. Am. Chem. Soc.,* 1934, **56**, 658.
48 A. Tenerz, I. Lonnberg, C. Berne, G. Nilsson and J. Leppert, *Eur. Heart J.*, 2001, **22**, 1102.
49 X.D. Yan, X.H. K. Xu and H.F. Ji, *Anal. Chem.,* 2005, **77**, 6197.
50 A. Antony, Blood, 1992, **79**, 2807.
51 I.G. Campbell, T.A. Jones, W.D. Foulkes and J. Trowsdale, *Cancer Res.,* 1991, **51**, 5329.

Graphical abstract

A nanosized porous PB/MIL-101(Fe), was facicly prepared with a uniform octahedral structure by growthing Prussian blue(PB) on microporous metal–organic framework MIL-101(Fe). It showed efficient intrinsic peroxidase-like activity, providing a simple and sensitive colorimetric assay to detect H_2O_2. This assay can offer more active sites and pore for peroxidase substrates and thus show satisfying performance for the sensing detection of H_2O_2(see graphic; TBM = 3,3',5,5'-tetramethylbenzidine).